Validation of a Model for Multiple Agglomeration

Ana Cameirão, Fabienne Espitalier, René David, Loïc Rouleau

Validation of a Model for Multiple Agglomeration

By *Ana Cameirão*, *Fabienne Espitalier**, *René David*, and *Loïc Rouleau*

A two-step agglomeration model is developed for the crystallization of a zeolite. It accounts for the crystallization of crystallites from the amorphous phase and the subsequent growth and agglomeration processes. The model explains the morphology of agglomerates with multiple structures, which were obtained. When porosity of the secondary agglomerates is introduced in the model, the agreement with experimental data is largely improved.

1 Introduction

Several crystallization products exhibit multiple levels of agglomeration: basic crystallites are embedded in primary agglomerates which, in turn, are reagglomerated in secondary agglomerates. The structure properties like porosities or sizes of the different levels of these particles influence their properties of use like catalytic performances or flowability.

A previous work [1] dealt with the hydrothermal autoclave crystallization of a zeolite from a gel containing amorphous particles. After pouring the reactants into the autoclave vessel, heating up to 150–200 °C was started. Then, the transformation into crystallites and the consecutive growth and agglomeration of these crystallites required about 72 hours to be completed. Chemical composition, stirring speed, temperature and ripening of the gel were varied. Final crystal size distributions, the desupersaturation profile and the crystallinity index against time were monitored.

2 Generation of Crystallites

Crystallites were supposed to be generated from amorphous particles with size L_0 and volume v_0 from surface contamination by a shrinking core model. This process starts at t_0. The conversion into a crystallite is completed within t_{con}. The amorphous volume v_a and the amorphous surface A_a are related by[1]:

$$\frac{dv_a}{dt} = -\frac{L_0}{2t_{con}} A_a \qquad (1)$$

---

[*]   A. Cameirão, F. Espitalier (espitali@enstimac.fr), R. David, Laboratoire de Génie des Procédés des Solides Divisés, CNRS-Ecole des Mines d'Albi – Carmaux, F-81013 Albi Cedex 9, France; L. Rouleau, Catalysis and Separation Department, IFP-Lyon, BP 3, F-69390 Vernaison, France.
1)   List of symbols at the end of the paper.

By integration of Eq. (1) one obtains the crystalline volume v_c:

if: $t < t_0$: $\qquad v_c = 0 \qquad (2)$

if $t_0 \leq t \leq t_0 + t_{con}$:

$$\frac{v_c}{v_0} = 1 - \left[1 - \frac{(t - t_0)}{t_{con}} \right]^3 \qquad (3)$$

if $t > t_0 + t_{con}$: $\qquad v_c = v_0 \qquad (4)$

t_0 is different for each amorphous particle and is assumed to follow a Gaussian distribution with the mean value $\bar{t}_0$ and the standard deviation σ.

$$p(t_0) = \frac{1}{\sigma\sqrt{2\pi}} \exp\left(-\frac{(t_0 - \bar{t}_0)^2}{2\sigma^2} \right) \qquad (5)$$

The ratio between the total crystalline volume V_c and the initial amorphous volume V_0 is:

$$\frac{V_c(t)}{V_0} = \int_0^t p(t_0) \frac{v_c}{v_0}(t, t_0) dt_0 \qquad (6)$$

The crystallinity index V_c/V_0 was experimentally monitored against the time from the samples by X-ray diffraction (see Fig. 1). As an amorphous particle with an external crystalline layer can start to agglomerate, the nucleation rate of crystallites will be proportional to the surface contamination and the initial concentration of amorphous particles.

$$r_N = N_{A0} p(t) \qquad (7)$$

t_0 and t_{con} were calculated from the starting time t_{start} of the experimental curve V_c/V_0 (see Fig. 1): no amorphous

particle begins to transform before $\bar{t}_0 - 2\sigma$; thus, for the entire suspension it is assumed that:

$$\bar{t}_0 = t_{start} + 2\,\sigma \qquad (8)$$

The half-life time t_{50} of an amorphous particle is derived from Eq. (3):

$$t_{50} = t_0 + \frac{t_{conso}}{4.85} \qquad (9)$$

For the complete set of amorphous particles, the half-life time is approximated as:

$$\bar{t}_{50} = \bar{t}_0 + \frac{t_{conso}}{4.85} \qquad (10)$$

Then, by fitting σ it is possible to simulate the crystallinity index V_c/V_0 against the time via Eqs. (2–6), (8), and (10); t_{con} was found identical for all experiments and equal to 3.1 h. Values of $\bar{t}_0$ and σ are reported in Tab. 1 for some typical runs. Runs 1 and 2 were done under the same chemical and stirring conditions, except a ripening period after reactant mixing, but before heating for run 2. Run 3 was conducted under different chemical (alkalinity) and stirring conditions as runs 1 or 2 and without ripening. All the runs were done at the same temperature.

$\bar{t}_0$ is influenced by alkalinity and ripening and by stirring speed, whilst σ is very sensitive to ripening and alkalinity and less to the stirring speed. The crystallinity curve of the particulate mass against time (see Fig. 1) fits experimental results extremely well when using this assumption.
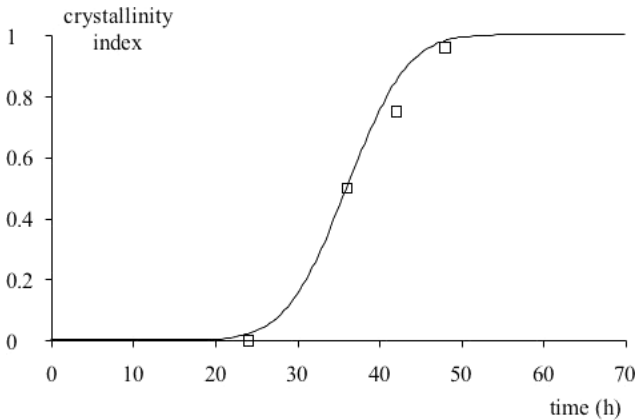

Figure 1. Cristallinity index against time for run 3.

Table 1. Values of parameters obtained for three typical runs at the same temperature (for the entire sets of experimental conditions see [1] and [2]).

	Run 1	Run 2	Run 3
σ [h]	6.5	8.8	5.7
$\bar{t}_0$ [h]	37	41	35

3 Agglomeration Model

A complete model [2] of the multiple agglomeration of the zeolite was set up. Crystal agglomeration starts when the particle surface is crystalline and follows a three-step process (see Fig. 2); First, collision of agglomerates or individual particles takes place and results in a labile aggregate, which may undergo either disruption or consolidation by crystal growth. It is generally accepted that the collision rate r_{col} is size-dependent and linked to the concentrations of colliding species:

$$r_{col} = K_{col}(S_i, S_j)\, N_i N_j \qquad (11)$$

where K_{col} depends on the collision regime (Brownian if mother crystal sizes < Batchelor scale, or laminar shear if Kolmogoroff scale > mother crystal sizes > Batchelor scale) encountered by the colliding particles:

$$K_{col,B} = 2kT(S_i + S_j)^2/(3\mu\, S_iS_j);$$
$$K_{col,L} = 0.16\,(P/\nu)^{1/2}(S_i + S_j)^3 \qquad (12)$$

Note that $K_{col,L}$ increases with the stirring power whereas $K_{col,B}$ is not stirring power dependent. If both particles to agglomerate are of the same size S, $K_{col,L}$ varies as S^3 and $K_{col,B}$ is size-independent. When keeping the largest size S_i constant one can observe that $K_{col,B}$ has a minimum for $S_j = S_i$, whereas $K_{col,L}$ reaches its maximum value for $S_j = S_i$. If the disruption of the aggregate and the crystal growth are independent processes and of first order with respect to the aggregate number concentration (i.e., not consecutive to further collisions), the agglomeration rate is the collision rate times an efficiency factor η [2].

$$r_{aggl} = r_{col}/(1 + k_d/k_c) = \eta\, r_{col} \qquad (13)$$

If the crystal growth rate is high, this efficiency factor is close to 1. By contrast, with low growth rates:

$$\eta \sim G/(k_d S_j) \qquad (14)$$

A reasonable assumption for η_B would be to consider k_{dB} as constant. Recently, Liew et al. [3] proposed an expression for k_{dL}:

$$k_{dL} \sim \rho_L P S_i/(\sigma^* L^*) \qquad (15)$$

which leads to:

$$\eta_L = AG/(PS_iS_j) \qquad (16)$$

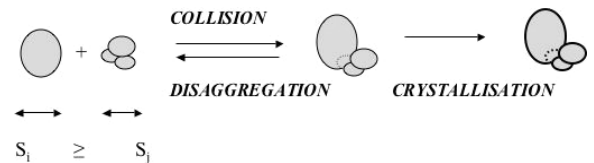where the constant A stands for both, liquid and solid properties.

Figure 2. Processes involved in crystal agglomeration.

Summarizing, for a given growth rate $r_{aggl,B}$ is not dependent on P, it is proportional to the common size S^{-1}, and it is minimum for agglomeration of particles of the same size. During size enlargement, agglomerations of small and large particles are thus favored (snowball effect), but the rate of agglomeration diminishes with size increase.

Conversely, $r_{aggl,L}$ is a decreasing function of P and is proportional to the common size if $S_j = S_i$. At constant S_i it is maximum for $S_j = \lambda_B$, minimum for agglomeration of particles of $S_j = S_i/3$, and reaches a weak secondary maximum at $S_j = S_i$. During size enlargement, if $S_i \gg \lambda_B$, agglomerations of particles of very different sizes are thus favored but, if S_i is of the same order of magnitude as λ_B, the rate of agglomeration becomes quasi-independent of the particle size. In several experiments size-independent agglomeration was observed [4]. Globally, the agglomeration rate is enhanced by size increase. Anyway, the agglomeration rate depends on supersaturation via G. When the supersaturation decreases, agglomeration, which is then mainly is laminar, becomes more and more difficult. It is thus expected that agglomerates formed under Brownian and laminar shear regimes show different morphologies.

Agglomeration is modeled like a set of stoichiometric chemical reactions between particle classes [2]. The stoichiometric coefficients are designed in order to account for both mass conservation and disappearance of one particle per agglomeration.

However, the method described in [2] was improved in this paper by including a liquid volume v_l into the apparent volume of the newly formed agglomerate:

$$a\, v_j + b\, v_i + v_l \rightarrow c\, v_m \qquad (17)$$

This allows one to predict the external porosity of the agglomerates, which was observed experimentally (see Fig. 3). The coefficients a, b, c, and v_l are given in Tab. 2.

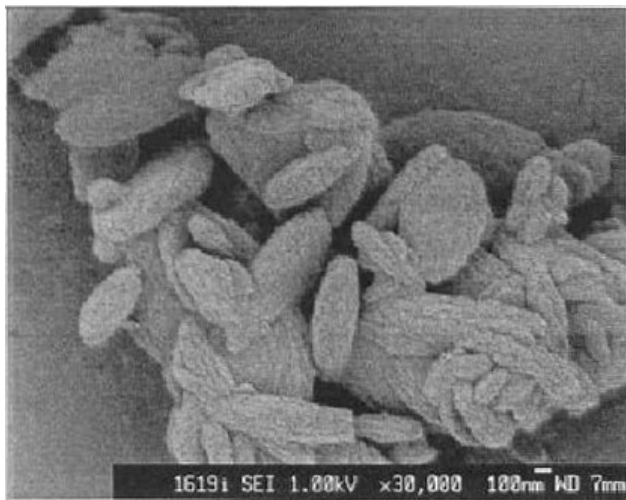**Table 2.** Stoichiometric coefficients and included liquid volume (see Eq. (17)) as functions of agglomeration classes i and j ≤ i.

a	j	b	c	Class m of agglomerate without porosity	Class m agglomerate with porosity	$v_l = cv_m - av_j - bv_i$
1/2	i	1/2	1/2	i+1	i+2	v_i
1	i–1	1/2	1/2	i+1	i+1	0
4/3	i–2	1	4/3	i	i+1	$4v_i/3$
8/7	i–3	1	8/7	i	i+1	$8v_i/7$
$v_i/(v_i-v_j)$	j < i–3	1	$v_i/(v_i-v_j)$	i	i	0

Then, the porosity is calculated as a function of time: It is the ratio of the mean trapped liquid volume $\overline{v}_l$ per unit of suspension volume to the total apparent solid volume concentration.

$\overline{v}_l$ is calculated by integrating Eq. (18) for all interactions (i, j) and their consequences for particle classes ranging from n = 1 to n_c:

$$\frac{d\overline{v}_l}{dt} = \sum_{n=1}^{n_c} \sum_{i=1}^{n_c} \sum_{j=1}^{i} v_l r_{aggl}(i,j,n,t) \qquad (18)$$

All other equations of the model can be found in [2].

4 Results and Discussion

The calculations of the model developed above were done with the same parametric values as in [2]. The agreement obtained with the experimental agglomerate size distribution is better (see Fig. 4). Note that the laser particle sizer measures apparent external dimensions of the agglomerates including external porosity between the primary agglomerates (see Fig. 3). Two codes, both based on backward differentiation, were used: LNAG did not use a numerical Jacobian matrix, whilst LSODE does, yielding similar results. The quality of
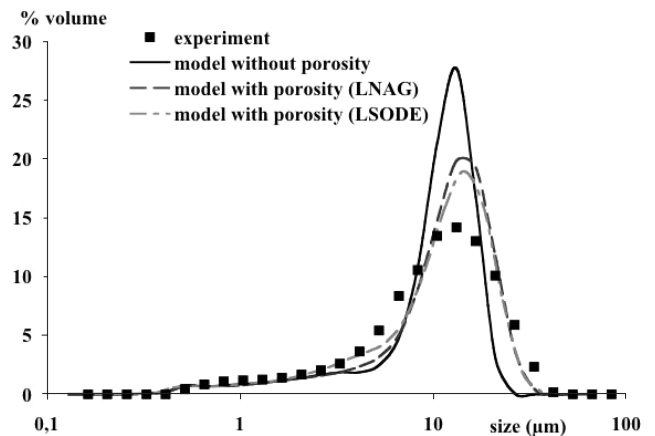

Figure 3. SEM picture of synthesized zeolite.

Figure 4. Apparent experimental and calculated particle size distributions with porosity modeling for run 3 using two different codes.

the agreement is much better than the one resulting from a previous model [2], but the model does not completely fit the experimental size distribution. In fact, Tab. 2 is a very crude approach of external porosity: a finer tuning of the daughter classes of the agglomerates is necessary.

5 Conclusions

The agglomeration process during crystallization is far from being completely understood. The crystalline growth is a key feature of this process, which makes the major difference with colloidal aggregation by playing the role of sticking particles. In some cases like the present one, the agglomeration becomes the dominant size enlargement process, more than crystal growth. The building-up of the final particle structure from the basic crystallites is often made of several agglomeration steps. Finally, efficient models of agglomeration must consider the importance of taking external porosity, especially for secondary agglomerates, when applicable, into account.

Acknowledgement

Symbols used

A	$[m^3 s^{-2}]$	constant
A_a	$[m^2]$	amorphous surface
a, b, c	$[-]$	stoichiometric coefficients
k	$[J\,molecule^{-1}K^{-1}]$	Boltzmann constant
k_c	$[s^{-1}]$	consolidation rate constant
k_d	$[s^{-1}]$	disruption rate constant
K_{col}	$[m^3 s^{-1}]$	collision rate constant
G	$[m s^{-1}]$	crystal growth rate
L	$[m]$	particle size
L^*	$[m]$	length of contact line
L_0	$[m]$	initial amorphous particle size
N_{A0}	$[m^{-3}]$	initial concentration of amorphous particles
N_n	$[m^{-3}]$	concentration of particles belonging to the class n
$p(t_0)$	$[s^{-1}]$	Gaussian distribution of beginning times
$p(t)$	$[s^{-1}]$	Gaussian distribution of times
P	$[W\,kg^{-1}]$	dissipated energy par unit mass
r_{aggl}	$[m^{-3}s^{-1}]$	agglomeration rate
r_{col}	$[m^{-3}s^{-1}]$	collision rate
r_N	$[m^{-3}s^{-1}]$	nucleation rate of crystallites
S_i	$[m]$	particle size of class i
S_j	$[m]$	particle size of class j
t	$[s]$	time
t_0	$[s]$	beginning of crystallites generation
$\bar{t}_0$	$[s]$	mean value of Gaussian distribution of t_0
t_{start}	$[-]$	starting time of the experimental curve
t_{con}	$[s]$	conversion time of one crystallite
t_{50}	$[s]$	half-life time of an amorphous particle
T	$[K]$	temperature
v_0	$[m^3]$	initial amorphous volume
v_a	$[m^3]$	amorphous volume
v_c	$[m^3]$	cristalline volume
v_l	$[m^3]$	trapped liquid volume
$\bar{v}_l$	$[m^3]$	mean trapped liquid volume
v_i, v_j, v_k	$[m^3]$	particle volume
V_0	$[m^3]$	initial amorphous volume
V_c	$[m^3]$	total crystalline volume
V_c/V_0	$[-]$	cristallinity index
σ	$[s]$	standard deviation of Gaussian distribution of t_0
σ^*	$[Pa]$	yield stress
λ_B	$[m]$	Batchelor microscale
λ_K	$[m]$	Kolmogoroff microscale
ρ_l	$[kg\,m^{-3}]$	liquid density
η	$[-]$	efficiency factor
ν	$[m^2 s^{-1}]$	kinematic viscosity
μ	$[kg\,m^{-1}\,s^{-1}]$	dynamic viscosity

Subscripts

B	Brownian
L	laminar
i, j, m, n, n_c, k	particle classes

References

[1] R. David, A. M. Paulaime, F. Espitalier, L. Rouleau, *Powder Technol.* **2003**, *130*, 338.

[2] R. David, F. Espitalier, A. Cameirao, L. Rouleau, *Kona* **2003**, *21*, 40.

[3] T. L. Liew, J. P. Barrick, M. J. Hounslow, *Chem. Eng. Technol.* **2003**, *26*, 282. DOI: 10.1002/ceat.200390042

[4] J. P. Andreassen, M. J. Hounslow, *AIChE J.* **2004**, *50*, 2772.